FERROELECTRICS
2018, VOL. 533, 99–107
https://doi.org/10.1080/00150193.2018.1470819

Taylor & Francis
Taylor & Francis Group

Structural and microstructural analyses on Sm-modified $BaTiO_3$ obtained from the Pechini's method

M. A. Oliveira[a,b], Y. Mendez-González[c], J. C. M'peko[d], A. C. Hernandes[d], R. Guo[e], A. S. Bhalla[e], and J. D. S. Guerra[a]

[a]Grupo de Ferroelétricos e Materiais Multifuncionais, Instituto de Física, Universidade Federal de Uberlândia, Uberlândia, Minas Gerais, Brazil; [b]Departamento de Física e Química, Universidade Estadual Paulista, Ilha Solteira, Sao Paulo, Brazil; [c]Facultad de Física–Instituto de Ciencia y Tecnología de Materiales, Universidad de La Habana, Vedado, La Habana, Cuba; [d]Grupo de Nanomateriais e Cerâmicas Avançadas, Instituto de Física de São Carlos (IFSC), Universidade de São Paulo, São Carlos, Sao Paulo, Brazil; [e]Multifunctional Electronic Materials and Devices Research Lab, Department of Electrical and Computer Engineering College of Engineering, The University of Texas at San Antonio, San Antonio, Texas, USA

ABSTRACT

Barium titanate ($BaTiO_3$) ceramics, prepared by the Pechini's method, were investigated considering the influence of the samarium-modifier concentration. Nanosized crystallites in the order of 15–20 nm have been successfully obtained by this synthesis process. The structural properties analyzed from the X-ray diffraction technique, confirmed a single ferroelectric phase with no additional secondary-phases, and suggest the amphoteric character (A- or B-site occupancy) of the Sm^{3+} ion into the $BaTiO_3$ structure. This effect, which has not been previously reported, has been also confirmed from microstructural (scanning electron microscopy) analysis. The obtained results reveal to be the starting point for further detailed investigations of the real amphoteric behavior of the Sm^{3+} ion, and other rare-earth elements in perovskite-type structure systems.

ARTICLE HISTORY
Received 5 September 2017
Accepted 20 February 2018

KEYWORDS
Pechini's method; nano-powders; $BaTiO_3$

1. Introduction

Barium titanate (BT) is an important perovskite type electro-ceramic material that still provides up today very important properties for various applications [1]. The excellent physical properties, in particular the dielectric response (high dielectric permittivity values and low dielectric losses) allow BT to be used in the manufacture of electronic devices such as multilayer ceramic capacitors (MLCs) [2,3]. On the other hand, the increasing interest to modify the BT compound with some iso- and/or hetero-valent ions has become a technologically important issue because of the increase in the application range of such materials, such as piezoelectric devices, thermistors components as well as semiconductor devices [4]. The addition of dopant elements into the $BaTiO_3$ perovskite structure causes structural deformations and defects formation, thus promoting significant changes in the physical properties [5].

CONTACT J. D. S. Guerra ✉ santos@ufu.br

Several researches on modified $BaTiO_3$ compounds have already been reported in the literature [6–10]. Anomalous effects are observed as a result of doping with donor elements (i.e. rare-earths) or pentavalent ions (i.e. niobium, tantalum), promoting very peculiar characteristics in their electrical and dielectric properties, which have not been yet fully understood [7–10]. For instance, semiconductor characteristics could be induced in BT ceramics by addition of La^{3+}, Er^{3+} or Gd^{3+} elements in the Ba-site as well as the Ta^{4+} or Nb^{5+} incorporation in the Ti-site of BT [7–10], and the properties of these materials can be controlled either by doping concentration or compositional substitutions. An interesting feature presented by semiconductor BT materials is the positive temperature coefficient of resistivity (PTCR) effect, which allows this system to be used as a thermistor component for thermal-switch devices [11]. The PTCR effect in such materials has been commonly associated to grain boundary phenomena [12], and some other aspects related to physical and chemical mechanisms, which govern anomaly in the resistivity need still to be further investigated in order to better understand the real nature of the observed behaviors. Most of the useful properties of BT-based ceramics are governed by the microstructural characteristics (i.e. grain-size) and, therefore, the control of homogeneous grain-growth in the material represent an essential and useful task for technological applications. Although the BT system has been extensively investigated for several decades long, there still exist new effects that remain unclear and need to be explored in detail.

Various synthesis methods have been explored in order to improve the structural, dielectric and electrical properties of BT, considering the inclusion of doping elements in the A- and/or B-site as well as solid-solutions formation [13–17]. However, significant advantages of the Pechini's method over the conventional solid-state reaction process (and others synthesis methods), which include lower synthesis temperatures and contaminations levels, higher stoichiometric control, better homogenization and density, and the possibility for obtaining nano-metric scaled powders [17], make it a potential route for obtaining materials with optimized properties. The aim of the present work is to investigate the structural and microstructural properties of $BaTiO_3$ ceramics modified with samarium (Sm^{3+}) ions obtaining by the Pechini-method. In particular, the influence of the Sm^{3+} content has been taken into account suggesting the ability of incorporation into the A- and B-site of the perovskite structure.

2. Experimental procedure

$Ba_{1\text{-}x}Sm_xTiO_3$ ($x = 0$, 0.001, 0.002, 0.003 and 0.005) stoichiometric ceramics were prepared by the polymeric precursor method based on the Pechini's route. Firstly, titanium citrate solution was prepared by dissolving citric acid ($C_6H_8O_7$, 99.5%, Synth) in titanium (IV) isopropoxide ($Ti[OCH(CH_3)_2]_4$, Sigma-Aldrich) at 60 °C with constant stirring, thus producing a homogenous solution. Simultaneously, samarium oxide (Sm_2O_3, 99.9%, Alfa Aesar) was dissolved in nitric acid solution (HNO_3, 65.0%, Quimis) at 60 °C, until forming a clear and transparent solution. Afterwards, barium acetate ($Ba(CH_3COO)_2$, 99.0%, Synth) was dissolved in citric acid with water as solvent at 60 °C and then, the samarium oxide solution and titanium citrate were added until the formation of a homogenous solution. The $P_H = 6$ was controlled by adding ammonia

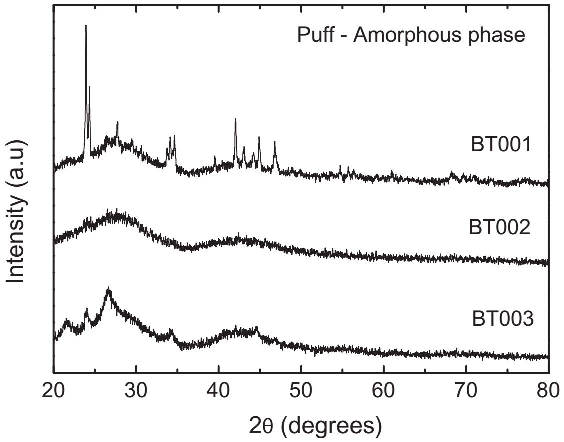

Figure 1. X-ray diffraction patterns, at room temperature, for BT001, BT002 and BT003 compositions in the amorphous phase.

hydroxide (NH_3OH) and finally ethylene glycol ($HOCH_2CH_2OH$, 99.0%, Synth) was dissolved in the previously formed solution in order to promote the polymerization. The obtained solution was then heated at 120 °C in order to remove the water and to promote the homogenization. After this process, the solution was heated at 400 °C for 4 hours to form the polymeric stable resin, which become an amorphous phase powder (called "puff") after thermal treatment. The calcination was performed at 700 °C for 2 hours in order to remove organic compounds and to promote the reaction between of the constituent materials. The calcined powders were pressed at 2.0 MPa (uniaxial pressing) and 200 MPa (isostatic pressing). The sintering procedure was carried out at 1300 °C for 2 hours.

The X-ray diffraction (XRD) experiments were carried out, at room temperature, using a Rigaku Ultima IV diffractometer with CuKα radiation in the 2θ range of 20–80°. Microstructural properties were carried out from scanning electron microscopy (SEM) using an Evo-SL15 microscope. The samples were hereafter labeled as BT, BT001, BT002, BT003 and BT005 for Sm concentrations of $x = 0$, 0.001, 0.002, 0.003 and 0.005, respectively.

3. Results and discussion

In order to analyze how the thermal treatment influences the crystal structure of the studied compositions, the structural properties were investigated from the XRD profiles obtained throughout the involved stages during the preparation process of the samples. Fig. 1 shows the XRD patterns for the obtained powders ("puff") by heating the precursors at 400 °C for 4 hours, for some of the studied compositions. In order to confirm the beginning of the crystallization process, three compositions (BT001, BT002 and BT003) were selected. It can be observed that the thermal treatment carried out for the "puff" formation causes the formation of the expected amorphous phase for the obtained powders. As can be seen in Figure 1, the results show few peaks for different reflections, which reveal the beginning of the crystallization process. This behavior indicates that the thermal treatment was carried out at a temperature value close to the

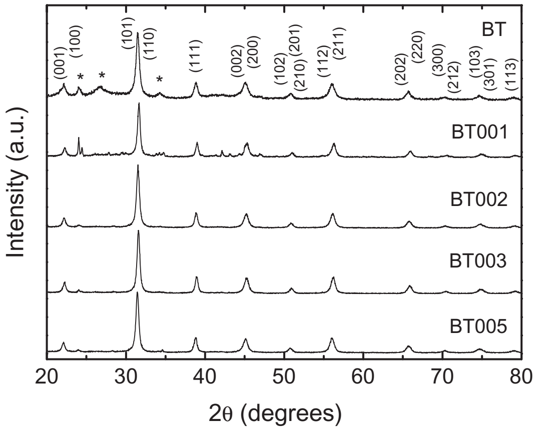

Figure 2. X-ray diffraction patterns, at room temperature, obtained on calcined powders for barium titanate (BT) and BT001, BT002, BT003 and BT005 compositions. The indexation is the same for all compositions. The peaks marked with an asterisk (*) were identified as $BaCO_3$ phase.

ideal temperature, before the total crystallization process, thus suggesting that the calcination procedure can be performed from the obtained amorphous phase "puff", which indeed can be used as the precursor powder.

Room temperature XRD patterns, obtained in the calcined powders, are show in Figure 2 for pure BT and BT001, BT002, BT003 and BT005 compositions. The diffraction peaks were indexed according to the ICSD database (No. 15453) for the BT compound [18] and the indexation is the same for all compositions. As observed, the heat treatment performed at 700 °C for 2 h resulted in the formation of the majority perovskite phase for all the compositions. It is well known that barium titanate powders to be synthetized may reach a higher chemical homogeneity, when compared to conventional mixed oxides synthesis processes. However, for the studied compositions, it can be observed the formation of a minority phase (indicated with asterisk) with typical reflections corresponding to the barium carbonate ($BaCO_3$) in the 2θ range of 25°–30° and $2\theta = 34°$. The residual $BaCO_3$ phase is created during the homogenization process with the citric acid in the formation of the final compound, showing that the reaction has not been completed after the calcination process, even though the perovskite phase has been already obtained.

On the other hand, the results shown in Figure 2 reveal broad diffraction peaks, thus indicating the nanometric characteristic of the post-calcined particles [19], which in fact have been confirmed from the microstrutural analysis by using the Williamson-Hall's method [20]. Results revealed nanosized crystallites in the order of 15–20 nm, which is in agreement with the reported results in the literature for the BT system doped with other elements [21]. Therefore, we can conclude that the Pechini's method was efficient to obtain nano-powder barium titanate, which is very important factor in the manufacture of nano-structured materials for application in high-integration level electronic components. According to the obtained results for the calcined samples, no shift in the peaks position was observed for doped compositions (BT001, BT002, BT003 and BT005), when compared with pure BT sample, indicating that the addition of Sm^{3+} ions was not enough to modify the $BaTiO_3$ perovskite structure during the calcination

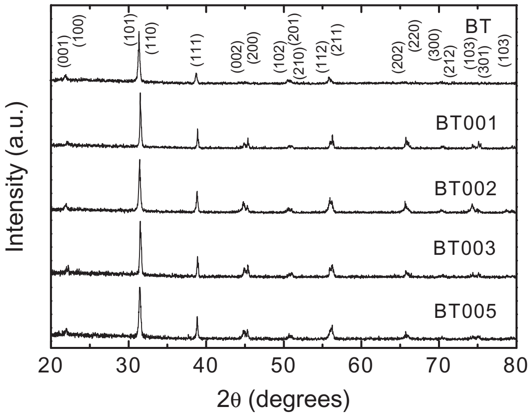

Figure 3. The X-ray diffraction patterns, at room temperature, obtained on the sintered samples for barium titanate (BT) and BT001, BT002, BT003 and BT005 compositions. The indexation is the same for all compositions.

process. The higher densification of the studied ceramics can be achieved after the final sintering process.

Figure 3 shows the room temperature XRD patterns for pure BT and BT001, BT002, BT003 and BT005 sintered ceramics. A distorted tetragonal perovskite structure with *P4mm* space group was confirmed for all the cases. The diffraction peaks were again indexed according to the ICSD database (No. 15453) for the $BaTiO_3$ compound [18] and the indexation is also the same for all compositions. Different to the calcination process, no trace of secondary phases ($BaCO_3$) was observed after the sintering process, which indicates that the high solubility of the Sm^{3+} ion into the BT crystalline lattice to form a homogeneous solid-solution.

However, a significant structural change of the XRD profile has been observed with the increase of the samarium content for 2θ in the ranges of 31.4–31.6°, corresponding to the (101) reflection. This result can be observed in the Figure 4, which show the composition (x) dependence of 2θ for the (101) reflection. It can be observed that the peak position increases between from the pure BT up to the BT003 composition ($0 \leq x \leq 0.003$) and then decreases for the BT005 composition ($x = 0.005$). This behavior can be interpreted in terms of the amphoteric character of the doping element, which can occupy both A- and B-sites in the perovskite structure of the $BaTiO_3$ system. According to the results reported in the literature rare-earth ions with ionic radii (IR) between 0.87 Å and 0.94 Å could reveal some amphoteric character, which in fact strongly depends of the doping concentrations [22]. It is well known that, according to the Bragg's law [23], an increase in the (101) reflection angle, which corresponds to the maximum intensity peak, leads to a decrease in the interplanar distance (d) and hence a decrease in the volume of the unit cell is expected. In this context, the shift observed for the (101) reflection angle, from lower to higher values, can be explained due to a structural contraction of the unit-cell attributed to the substitution of a larger ionic-radius element (IR_{Ba2+}=1.61 Å) by a smaller one (IR_{Sm3+}=1.24 Å) at the dodecahedral site (A-site) for BT001, BT002 and BT003 compositions [24]. Nevertheless, the decrease of the (101) reflection angle for the BT005 composition suggests a possible structural expansion of the unit-cell and, therefore, a partially substitution of a smaller ionic-radius

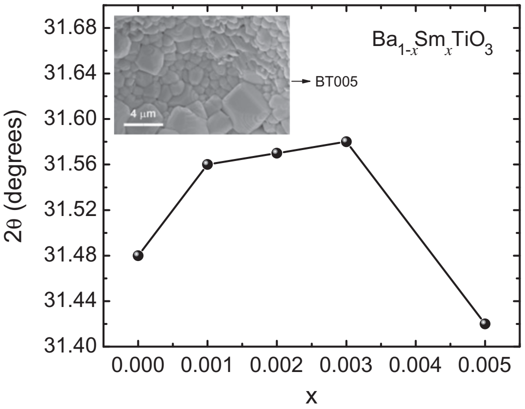

Figure 4. Dependence of the (101) reflection position on the samarium concentration (*x*) for all studied compositions. The upper left inset shows the SEM micrograph for the BT005 sample.

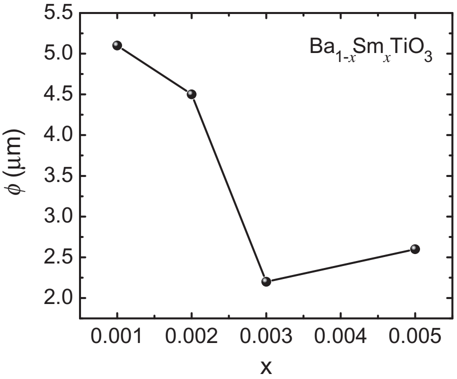

Figure 5. Dependence of the average grain-size (ϕ) on the samarium concentration (*x*) for BT001, BT002, BT003 and BT005 compositions.

ion (RI_{Ti4+}=0.61 Å) by a larger one (IR_{Sm3+}=0.96 Å) at the octahedral B-site of the structure [24]. Therefore, the obtained results for the XRD measurements suggest that the Sm^{3+} ion behaves as an amphoteric element with substitutional character in both Ba-site and Ti-site of the perovskite structure of the $BaTiO_3$ system. In order to obtain a detailed interpretation on the amphoteric character of the samarium ion, complementary measurements should be considered in further research for the studied ceramics.

The inset of Figure 4 shows the SEM image obtained for the BT005 ceramic, as example of the micrographs obtained for all the studied compositions, which reveals a highly dense microstructure with low porosity level and non-homogenous grain-size distribution. Figure 5 displays the composition (x) dependence of the average grain-size (ϕ). The ϕ values were obtained considering the SEM images for the BT001, BT002 and BT003 compositions (not shown here).

A decrease in the average grain–size (ϕ) with the increase of the Sm^{3+} content was observed for the compositions BT001, BT002 and BT003, exhibiting ϕ values between 5.1 μm and 2.2 μm. Previous researches have reported that the average grain–size strongly depends on the incorporation of the doping ions at the A- or B-sites of the perovskite structure [25], as well as to the formation of structural defects (i.e. vacancies) [26]. In this context, pinning effects at the grain boundary could be promoted with the increase of the Sm^{3+} ion concentration, thus inhibiting the grain-growth effect for lower doping concentrations (BT001, BT002 and BT003). On the other hand, an increase in the ϕ value for the BT005 sample, with respect to that obtained for the BT003 composition, was observed, which has been ascribed to the liquid phase formation in the grains boundaries for higher doping concentrations.

The process of the liquid phase formation has been studied, mainly for compounds which are obtained by the conventional sintering method. The presence of the liquid phase (formed during the heat treatment) promotes processes of dissolution of the involved ions into the liquid followed by mass transport from a grain to another one. This diffusion through the liquid phase favors a marked grains-growth, accompanied by expulsion of porosity and high densities of the sample at relatively low temperatures [27]. In the case of the $BaTiO_3$, the development of these processes is observed when the material is prepared for a Ba/Ti <1 ratio (i.e. considering small excess of TiO_2 in the initial formulation) with the presence of an eutectic point around 1320 °C [12]. For the studied compositions, the Ba/Ti ratio decreases from 0.999 (for $x = 0.001$) up to 0.995 (for $x = 0.005$) with the increase of the samarium content. This result favors the formation of a liquid phase, which leads to an anomalous average grain–size growth, forming regions with non-homogeneous grain-sizes as indeed has been observed in the inset of Figure 4 for the BT005 composition.

However, previous research reported in the literature has also associated the average grain-size effect to the incorporation of some rare-earth ions in the A- or B-site of the structure [28]. In this way, as previously reported by Li *et al.* [28], the decrease of the grain-size could be ascribed to the successful incorporation of the rare-earth elements (i.e. Eu^{3+}) into the A-site of the perovskite structure of the BT, thus promoting the high solubility of the doping element. Therefore, the obtained behavior in the grain-size for the higher composition investigated in the present work (BT005) could also suggest the incorporation of the samarium ion into the B-site of the structure, thus confirming the previous discussed XRD results on the $Ba_{1-x}Sm_xTiO_3$ samples and the possible amphoteric character of the Sm^{3+} ion.

In order to better clarify the observed amphoteric behavior for the Sm-modified BT system, which indeed has not been previously reported, additional and complementary measurements should be taken into account, involving not only structural properties considering Rietveld refinement but also electric and dielectric analyses. Such discussions are in progress and will be reported in further works.

4. Conclusions

Sm-modified barium titanate ceramics were synthesized by the polymeric precursor method, based on the Pechini's route. Microstructural analysis showed nanometric size, which confirm the efficiency of the Pechini's method to obtain nano-powders based barium titanate samples. The X-ray diffraction results, as well as scanning electron microscopy analysis, suggest the amphoteric character for the Sm^{3+} ion in the $BaTiO_3$

system, which has not been previously reported. Additional studies are being taken into account in other to confirm such amphoteric behavior and the obtained results will be discussed in further works.

Funding

Thanks to CNPq, FAPESP and FAPEMIG Brazilian agencies for financial support. MSc. Mendez-González acknowledges the receipt of the grant from the Abdus Salam International Centre for Theoretical Physics, Trieste, Italy. Dr. M. A. Oliveira also thanks the Materials Science Post-Graduate Program (PPGCM), UNESP, Ilha Solteira, Brazil.

References

1. F. Jona, and G. Shirane. *Ferroelectric Crystals*. New York: Dover Publications, Inc.; 1993.
2. M. Sayer, and K. Sreenivas. Ceramic thin films: fabrication and applications. *Science*. **247**(4946), 1056 (1990).
3. R. E. Cohen. Origin of ferroelectricity in perovskite oxides. *Nature*. **358**(6382), 136 (1992).
4. S. R. Syrtsov, *et al.*, Positive temperature coefficient of resistivity in thin films of barium titanate. *Mater. Sci. Semicond.* **5**(2–3), 223 (2002).
5. C. Kittel. *Introduction to Solid State Physics*. Berkeley: Wiley; 2005.
6. H. L. Wang. *Structure and Dielectric Properties of Perovskite-Barium Titanate (BaTiO3). Partial Fulfillment of Course Requirement for MatE 115*. San Jose: San Jose State University; 2002.
7. N. H. Chan, and D. M. Smyth. Defect chemistry of donor-doped $BaTiO_3$. *J. Am. Ceram. Soc.* **67**(4), 285 (2006).
8. F. D. Morrison, A. M. Coats, D. C. Sinclair, and A. R. West. Charge compensation mechanisms in la-doped $BaTiO_3$. *J. Electroceram.* **6**(3), 219 (2001).
9. T. Miki, A. Fujimoto, and S. Jida. An evidence of trap activation for positive temperature coefficient of resistivity in $BaTiO_3$ ceramics with substitutional Nb and Mn as impurities. *J. Appl. Phys.* **83**(3), 1592 (1998).
10. S. Urek, and M. Drofenik. PTCR behaviour of highly donor doped $BaTiO_3$. *J. Eur. Ceram. Soc.* **19**(6–7), 913 (1999).
11. S. Marković, *et al.*, Densification, microstructure, and electrical properties of $BaTiO_3$ (BT) ceramics prepared from ultrasonically de-agglomerated BT powders. *Mater. Manuf. Processes*. **24**(10–11), 1114 (2009).
12. J. Nowotny, and M. Rekas. Positive temperature coefficient of resistivity for $BaTiO_3$-based materials. *Ceram. Int.* **17**(4), 227 (1991).
13. M. N. Rahaman. *Ceramic processing and sintering*. New York: Marcel Dekker; 2003.
14. M. Kakihana. Sol-Gel preparation of high temperature superconducting oxides. *J. Sol-Gel. Sci. Technol.* **6**(1), 7 (1996).
15. J. Livage, M. Henry, and C. Sanchez. Sol-Gel chemistry of transition metal oxides. *J. Phys. Chem. Solids*. **18**(4), 259 (1988).
16. M. P. Pechini. Method of preparing lead and alkaline earth titanates and niobates and coating method using the same to form a capacitor. U. S. Patented 3,330,697, July 1967.
17. P. P. Phule, and S. H. Risbud. Low-temperature synthesis and processing of electronic materials in the BaO–TiO_2 system. *J. Mater. Sci.* **25**(2), 1169 (1990).
18. H. T. Evans Jnr. An x-ray diffraction study of tetragonal barium titanate. *Acta Cryst.* **14**(10), 1019 (1961).
19. A. C. F. M. Costa, *et al.*, Synthesis and characterization of TiO_2 nanoparticles. *Cerâmica*. **52**(324), 255 (2006).
20. G. K. Williamson, and W. H. Hall. X-ray line broadening from filed aluminium and wolfram. *Acta Metall.* **1**(1), 22 (1953).

21. S. Madolappa, R. Sagar, and R. L. Raibagkar. Synthesis, structural and electrical investigations of Gd-and Cr-doped $BaTiO_3$ nanoparticle ceramics. *Ferroelectrics*. **413**(1), 37 (2011).
22. Y. Tsur, T. D. Dunbar, and C. A. Randall. Crystal and defect chemistry of rare earth cations in $BaTiO_3$. *J. Eletroceram*. **7**, 25 (2001).
23. B. D. Cullity. *Elements of X-ray diffraction*. London: Addison-Wesley Publishing Company, Inc.;1967.
24. R. D. Shannon. Revised effective ionic radii and systematic studies of interatomic distances in halides and chalcogenides. *Acta Cryst. A*. **32**(5), 751 (1976).
25. T. Yamamoto, Y. Ikuhara, and T. Sakuma. Controlling microstructure and grain boundary structure in $BaTiO_3$. *Mater. Japan*. **38**(2), 126 (1999).
26. J. Daniels, and K. H. Hardtl. Electrical conductivity at high temperatures of donor-doped barium titanate ceramics. *Philips Res. Repts*. **31**, 489 (1976).
27. J. Nowotny, and M. Rekas. Defect chemistry of $BaTiO_3$. *Sol. State Ionics*. **49**, 135 (1991).
28. Y.-X. Li, X. Yao, X.-S. Wang, and Y.-B. Hao. Studies of dielectric properties of rare earth (Dy, Tb, Eu) doped barium titanate sintered in pure nitrogen. *Ceram Int*. **38**, S29 (2012).